Article

Optimal Operation of Networked Microgrids for Enhancing Resilience Using Mobile Electric Vehicles

Asfand Yar Ali [1], Akhtar Hussain [1,2], Ju-Won Baek [3] and Hak-Man Kim [1,2,*]

[1] Department of Electrical Engineering, Incheon National University, 12-1 Songdo-dong, Yeonsu-gu, Incheon 406-840, Korea; asfi1617@gmail.com (A.Y.A.); hussainakhtar@inu.ac.kr (A.H.)

[2] Research Institute for Northeast Asian Super Grid, Incheon National University, 119 Academy-ro, Yeonsu-gu, Incheon 22012, Korea

[3] Division of Smart Grid, Korea Electrotechnology Research Institute, Changwon 51543, Korea; jwbaek@keri.re.kr

[*] Correspondence: hmkim@inu.ac.kr; Tel.: +82-32-835-8769; Fax: +82-32-835-0773

Abstract: The increased intensity and frequency of natural disasters have attracted the attention of researchers in the power sector to enhance the resilience of power systems. Microgrids are considered as a potential solution to enhance the resilience of power systems using local resources, such as renewable energy sources, electric vehicles (EV), and energy storage systems. However, the deployment of an additional storage system for resilience can increase the investment cost. Therefore, in this study, the usage of existing EVs in microgrids is proposed as a solution to increase the resilience of microgrids with outages without the need for additional investment. In the case of contingencies, the proposed algorithm supplies energy to islanded microgrids from grid-connected microgrids by using mobile EVs. The process for the selection of EVs for supplying energy to islanded microgrids is carried out in three steps. Firstly, islanded and networked microgrids inform the central energy management system (CEMS) about the required and available energy stored in EVs, respectively. Secondly, CEMS determines the microgrids among networked microgrids to supply energy to the islanded microgrid. Finally, the selected microgrids determine the EVs for supplying energy to the islanded microgrid. Simulations have shown the effectiveness of the proposed algorithm in enhancing the resilience of microgrids even in the absence of power connection among microgrids.

Keywords: electric vehicles; energy management system; microgrid; networked microgrids; resilience; resilience enhancement

1. Introduction

Natural disasters result in power outages and economic loss to the electricity consumers [1]. The probability of occurrence of these natural disasters is low but the damage ratio is high, that is why they are known as low probability, high-impact events. However, the occurrence of these low probability high-impact events has increased in the past decades mainly due to climate change [2,3]. Therefore, the concept of resilience has gained much attention in the power system. Resilience is the ability of the system to resist, adapt, and timely recover from disruptions caused by natural disasters. To enhance the resilience of the power systems, various studies are conducted, including generalized resilience enhancement methods [4,5], and long/short term resilience of power systems [4,6]. Various solutions are proposed in these studies for resilience enhancement and the most common ones among them are the integration of distributed energy resources, microgrid formulation, and line hardening [7,8]. Microgrids resilience enhancement schemes gain popularity due to their ability to sustain the penetration of renewable resources and to withstand in the islanded mode.

Microgrids are usually used as a resource for the resilience enhancement of power systems during major outages. A microgrid can connect or disconnect from the utility grid to make it able to work in grid-connected and islanded modes [9,10]. In some cases, microgrids are connected to support the critical load of other microgrids having a shortage of power supply [11]. The resilience of power systems can be increased by transforming them into microgrids [12,13], or by forming networked microgrids [14]. Moreover, a battery energy storage system can also be used for enhancing the resilience of the power system. Similarly, parked electric vehicles (EVs) in microgrids and mobile battery energy storage systems are also considered as potential resilience resources [15–20].

EVs are increasing day by day due to reduction in manufacturing cost, advanced battery technology, and their environmental merits. According to [21], EV sales will reach 44 million vehicles per year by 2030. Therefore, EVs can play a vital role in the resilience of the microgrids. The author in [17] has used a shared parking lot for the resilience of two buildings together. In [22], the concept of EVs aggregator has been used to supply the energy in the case of any contingency in a multi-microgrid system. EVs charge and discharge their energy while parked in the parking lot. The concept to store additional energy in the batteries of the electric vehicles for the resilience of the islanded microgrid is discussed in [23].

Electric vehicles are moveable battery energy storage systems. Therefore, they can move from one place to another to supply energy. In [18,19], the concept of a movable battery energy storage system is used where the battery is mounted on the truck is used for resilience purposes and concept of the resilience of the microgrid system by routing the mobile energy storage system to the area where energy supply is required is used, respectively. The truck is moved to the outage area and the battery is used to fulfill the needs of the system in the contingency. However, the limitation behind this concept is that large capital investment is required to build a mobile battery energy storage system. The author of [23], tried to solve the problem by storing additional energy in the batteries of electric vehicles parked in the parking lot of the microgrid for the resilience of the system in the case of an outage. Therefore, additional capital investment for making a moveable battery is waved by the author. In [17,22], EVs parked in the parking lot of the multi-microgrid system are used for the system resiliency to go one step further ahead of the work in [23]. However, in [17], the limitation is that the microgrids should be in the same locality to share the same parking lot and should have a power connection with the shared parking lot. EVs are only used to survive the microgrid in which they are parked at the time of contingency. However, during emergencies, other microgrids having limited or no EVs could also face power disruptions which may ultimately result in the loss of critical loads.

In order to cope with the limitations mentioned in the above paragraphs, an attempt has been made in this study to solve the problem of resiliency in the multi-microgrid system. In our study, resilience is the ability of the system to survive against any contingency with the help of EVs. In contrast to the existing studies [18,19], where a huge investment is required to deploy an additional battery for resilience, existing EVs in the healthy microgrids can be used for enhancing the resilience of microgrids with a power outage in the proposed algorithm. Similarly, the microgrids having outages need not be physically connected with the healthy microgrids, which was a major assumption in [17,22]. Finally, by using the proposed methods, microgrids with a limited number of EVs can also enhance their resilience by feeding their critical loads via EVs of other microgrids. In order to achieve these goals, an optimization algorithm is proposed in this study to supply the energy to the islanded microgrid (lost connection from the system due to any contingency) from the grid-connected microgrid in the multi-microgrid system using electric vehicles. Electric vehicles from the healthy microgrid travel to the islanded microgrid to supply energy. This algorithm performs optimization in three steps as discussed in the upcoming sections of the paper.

2. System Model and Proposed Resilience Enhancement Method

2.1. System Model and Components of Multi-Microgrid System

A multi-microgrid system consisting of *K* microgrids (MGs) is considered in this study, where *K* is a finite number. Microgrids can share power with other microgrids in the network and can also trade power with the utility grid. MGs constitute dispatchable generators (DGs), a battery energy storage system (BESS), renewable distributed generation (RDG), EV parking lot, and electrical load. Switches on the power lines (S1, S2, etc.) determine the mode of the operation of the multi-microgrid system. During normal operation time, these switches are considered as closed, they are open for the microgrid having an outage due to any natural disaster.

A typical networked microgrid system shown in Figure 1 is optimized in a hierarchical way using microgrid energy management systems (MG-EMSs) and a central energy management system (CEMS). MG-EMS is responsible for the local level optimization of MGs. After optimization, MG-EMS sends information to CEMS, which is responsible for the global level optimization of the multi-microgrid system. CEMS performs optimization based on the information received from MG-EMSs.
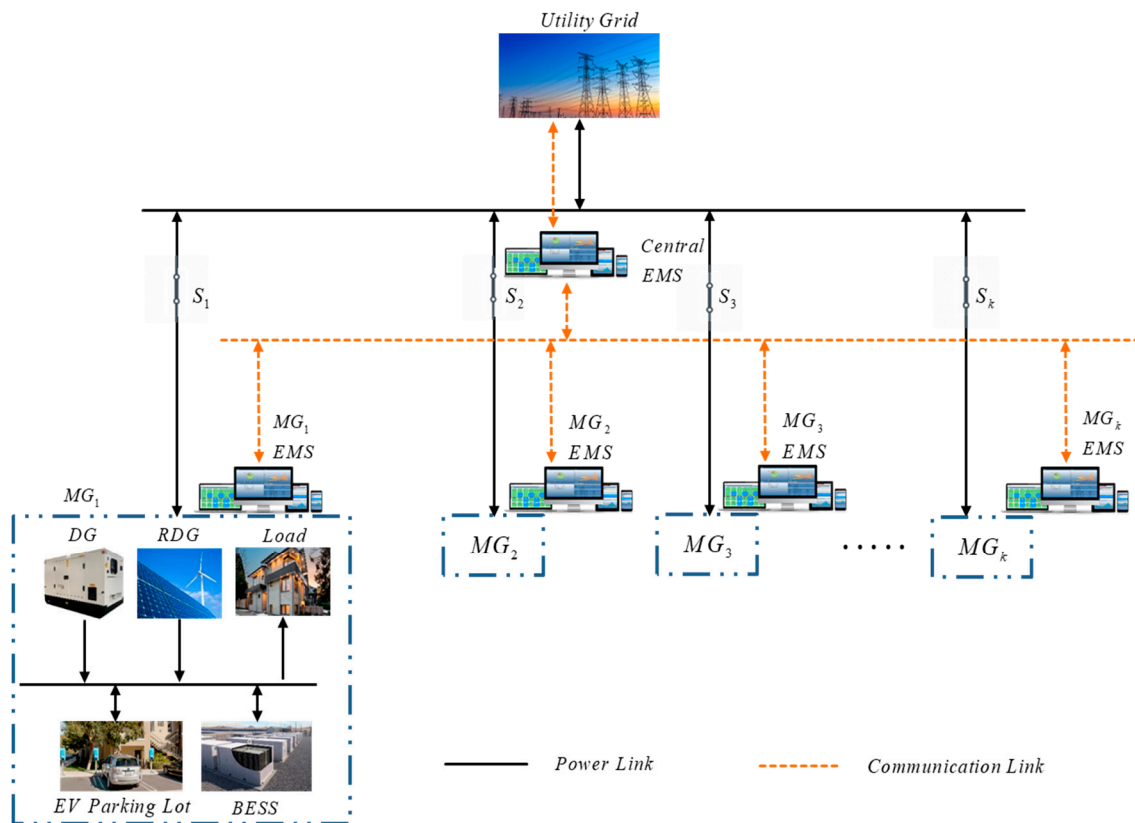

Figure 1. System model for a typical microgrid network.

2.2. Normal Mode

In normal mode, all the microgrids in the multi-microgrid system are in the grid-connected mode, i.e., can trade power with the utility grid, and can send/receive power to/from other microgrids of the multi-microgrid system. Optimization in the normal mode is performed as follows:

- Each microgrid is equipped with its own EMS, which is responsible for the local level optimization of the microgrid by utilizing the local resources. On the completion of

the local optimization, surplus and shortage power in the microgrid is informed to the central EMS at each interval of time.

- CEMS is responsible for global optimization. After receiving information from MG-EMSs and market price from the utility grid, it performs global optimization for minimizing the overall operation cost of the multi-microgrid network. CEMS decides the feasibility of sharing power among microgrids and/or trading power with the utility grid [24].

2.3. Proposed Resilience Enhancement Mode

This mode is proposed to enhance the resilience of the system in case of any contingency in the system. In case of any natural disaster, the power link between the microgrid and the network is lost. A microgrid that has lost the power connection with the networked in the time of contingency is considered an islanded microgrid. Grid-connected microgrids and islanded microgrids can perform their local level optimization in separate ways. Figure 2 shows the operation stages of resilience enhancement-mode at the time of contingency. During this mode, optimization is performed in two rounds, multi-microgrid (MMG) system resilience enhancement scheme and optimization of grid-connected microgrids. In the first round (left side of Figure 2), EV selection is carried out for the resilience enhancement of the islanded MG and is based on the optimized results from the last interval. In the second round, optimization of the grid-connection MGs is performed after the selection of the EVs. Details about each round are explained in the following sections.
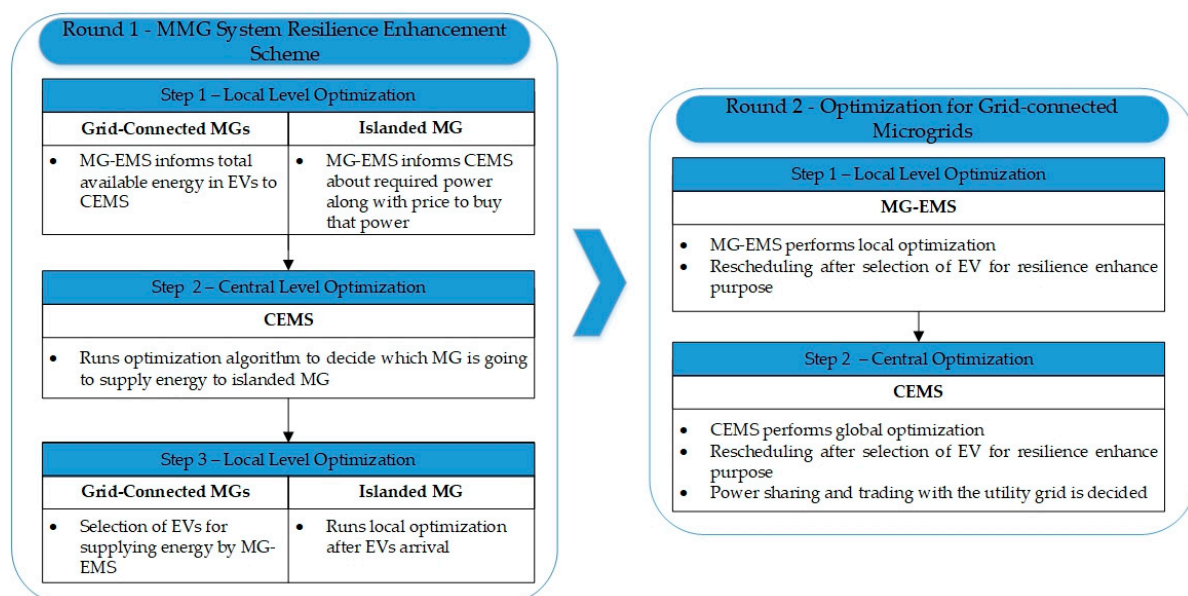

Figure 2. Operation stages of resilience enhancement mode.

2.3.1. Multi-Microgrid System Resilience Enhancement Scheme (Round 1)

In this round, the MMG system decides to supply energy to the islanded MG through EVs. In step 1, as shown in Figure 2, grid-connected MGs inform their total available energy to CEMS. Here total available energy refers to the energy available in the agreed EVs among the EVs parked in the parking lot. On the other hand, at the same time, islanded MG will inform its required power to CEMS through the communication link.

In the second step of round 1, as shown in Figure 2, CEMS performs a global level optimization for supplying the energy to islanded MG through grid-connected microgrids. This decision is based on the distance between microgrids in the multi-microgrid system. The closest microgrid in the vicinity of the islanded MG supplies the required energy

through EVs. This will reduce the energy consumption of EVs while traveling to and from the on-emergency microgrid.

In the third step of round 1, MG-EMSs make decisions based on the information given to them by CEMS. CEMS decides which MG is going to supplying energy in step 2, and MG-EMSs need to decide which EV should be sent for supplying energy to islanded MG. This decision is necessary when the total available energy in the microgrid is more than the required energy. In this way, the minimum number of EVs and most efficient EVs are chosen among agreed ones. By performing this optimization step, an optimal decision is made in choosing the EVs for resilience enhancement.

2.3.2. Optimization for Grid-Connected Microgrids (Round 2)

In the first round of the multi-microgrid system's resilience enhancement scheme, the EVs are selected for fulfilling the resilience demand of the islanded microgrid. Therefore, there is a need to reschedule the grid-connected microgrid in the system. In the first step of round 2, as shown in the right box of Figure 2, MG-EMSs perform the local level optimization as in the normal mode for the optimal operation of the microgrid. In this step, optimization is performed by considering those EVs which are going to leave the microgrid. On completion of optimization for one interval, grid-connected microgrids share their surplus and shortage power to CEMS. Surplus and shortage of power information are shared for global optimization. While in the second step, on receiving the information from the grid-connected MG-EMSs, CEMS performs global optimization. For grid-connected microgrids, CEMS will perform the same optimization as in normal mode by sharing power among microgrids and/or trading with the utility grid.

3. Problem Formulation

To realize an optimization problem for this multi-microgrid system, mathematical models are formulated in this section. Both normal and resilience enhancement modes are modeled to solve and minimize the operational cost as well as increase the resilience of the system. The developed model is based on mixed-integer linear programming (MILP). The scheduling horizon of the proposed model is T with the time interval t, which could be of any uniform interval of time.

3.1. Normal Mode

3.1.1. Microgrid Energy Management System

The proposed optimization model aims to minimize the total operational cost at the local level. The objective function of the local EMS is given in Equation (1). The first term shows the DG generation cost, the second term represents the price for buying power from the utility grid, and the third term shows the profit gained by selling power to the utility grid.

$$Min \sum_{t=1}^{T} (C^{DG} \cdot P_t^{DG} + C_t^{GB} \cdot P_t^{Short} - C_t^{GS} \cdot P_t^{Sur}) \tag{1}$$

Subjected to

$$P_{min}^{DG} \leq P_t^{DG} \leq P_{max}^{DG} \qquad \forall t \in T \tag{2}$$

$$P_t^{Short} + P_t^{DG} + P_t^{RDG} + P_t^{B-} + \sum_{v=1}^{V} P_{v,t}^{ev-} = P_t^{load} + P_t^{Sur} + P_t^{B+} + \sum_{v=1}^{V} P_{v,t}^{ev+} \quad \forall t \in T \tag{3}$$

$$SoC_{min}^{B} \leq SoC_t^{B} \leq SoC_{max}^{B} \quad \forall t \in T \tag{4}$$

$$0 \leq P_t^{B+} \leq P_B^{cap}(1 - SoC_{t-1}^{B})/\eta^c \quad \forall t \in T \tag{5}$$

$$0 \leq P_t^{B-} \leq P_B^{cap} \cdot SoC_{t-1}^{B} \cdot \eta^d \quad \forall t \in T \tag{6}$$

$$SoC_t^{B} = SoC_{t-1}^{B} + (\eta^c \cdot P_t^{B+} - P_t^{B-}/\eta^d)/P_B^{cap} \quad \forall t \in T \tag{7}$$

$$SoC_{min}^{ev} \leq SoC_{v,t}^{ev} \leq SoC_{max}^{ev} \quad \forall t \in [t_v^{arr}, t_v^{dep}], v \in V \tag{8}$$

$$0 \leq P_{v,t}^{ev+} \leq P_{v,cap}^{ev} \cdot (1 - SoC_{v,t-1}^{ev})/\eta^{ev+} \quad \forall t \in [t_v^{arr}, t_v^{dep}], v \in V \tag{9}$$

$$0 \leq P_{v,t}^{ev-} \leq P_{v,cap}^{ev} \cdot SoC_{v,t-1}^{ev} \cdot \eta^{ev-} \quad \forall t \in [t_v^{arr}, t_v^{dep}], v \in V \tag{10}$$

$$SoC_{v,t}^{ev} = SoC_{v,t-1}^{ev} + (\eta^{ev+} \cdot P_{v,t}^{ev+} - P_{v,t}^{ev-}/\eta^{ev-})/P_v^{cap} \quad \forall t \in [t_v^{arr}, t_v^{dep}], v \in V \tag{11}$$

$$SoC_{v,t}^{ev} \geq SoC_{\min} + E^{res} \quad \forall t \in [t_v^{arr}, t_v^{dep}], v \in V \tag{12}$$

$$SoC_{v,t^d}^{ev} = SoC_{v,t^{dep}}^{exit} \quad \forall t \in t_v^{dep}, v \in V \tag{13}$$

Equation (2) shows the operating bounds for the DG. Equation (3) shows the power balance of the microgrid which implies that power generation needs to be balanced with the power consumption in each interval. Charging, discharging, and SoC of BESS is controlled through the constraints given in Equations (4)–(7). Charging and discharging of BESS are carried out considering charging efficiency (η^c) and discharging efficiency (η^d) as in [25]. BESS has been taken as a load during the charging time and as an energy source during the discharging time. Equations (8)–(13) controls the charging, discharging, and SoC of electric vehicles while considering the charging efficiency (η^{ev+}) and discharging efficiency (η^{ev-}) of the battery of EV. The constraint in Equation (12) is the resilience constraint which makes sure that EVs parked in the parking lot will store energy for resilience (E^{res}) as in [26]. At the time of departure, each EV is charged to its targeted SoC (SoC_{v,t^d}^{ev}) as represented by Equation (13).

3.1.2. Central Energy Management System

The main objective of CEMS is to perform global optimization to minimize the total operation cost of the multi-microgrid system, based on the information received from MG-EMS about the surplus power and shortage power at the local level. The first term in the objective function given in Equation (14) represents the price for buying power from the utility grid and the second term shows the profit gained by selling power to the utility grid.

$$Min \sum_{k=1}^{K} \sum_{t=1}^{T} (C_t^{GB} \cdot P_{k,t}^{GB} - C_t^{GS} \cdot P_{k,t}^{GS}) \tag{14}$$

Subjected to

$$\sum_{k=1}^{K} \sum_{l=1}^{L} \sum_{t=1}^{T} P_{k \to l,t}^{Send} = \sum_{\substack{k=1 \\ k \neq l}}^{K} \sum_{l=1}^{L} \sum_{t=1}^{T} P_{l \leftarrow k,t}^{Rec} \quad \forall t \in T, k \in K, l \in L \tag{15}$$

$$P_{k,t}^{Send} + P_{k,t}^{GS} = P_{k,t}^{Sur} \quad \forall t \in T, k \in K \tag{16}$$

$$\sum_{\substack{l=1 \\ k \neq l}}^{L} P_{k \leftarrow l,t}^{Rec} + P_{k,t}^{GB} = P_{k,t}^{Short} \quad \forall t \in T, k \in K, l \in L \tag{17}$$

$$P_{k,t}^{Rec} = \frac{P_{k,t}^{Short}}{P_t^{T\_Short}} \cdot P_t^{T\_Sur} \quad \forall t \in T, k \in K \tag{18}$$

Internal power trading from one microgrid to another microgrid is represented in the power balance equation as shown in Equation (15). Equation (15) depicts that the total power sent from k microgrids needs to be equal to the total power received by l microgrids in the multi-microgrid system. Equation (16) constraints that the total power sent ($P_{k,t}^{sent}$) and sold ($P_{k,t}^{GS}$) by any microgrid k at the time interval t should be equal to the surplus power of the microgrid. Power received ($P_{k \leftarrow l,t}^{Rec}$) by microgrid k from any other microgrid l in network and power bought from the utility grid ($P_{k,t}^{GB}$) at time interval t is given by

Equation (17). Total surplus power in the multi-microgrid system is proportionally divided among microgrids with a shortage of power, as a constraint by Equation (18).

3.2. Proposed Resilience Enhancement Mode

In this mode, an algorithm to supply the energy to the islanded microgrid has been proposed. The energy is supplied to the islanded microgrid from grid-connected microgrids through EVs to achieve additional resilience. The energy supplied through the EVs is the energy requested by the islanded microgrid after utilizing its local resources (DG, RDG, parked EVs, and BESS).

3.2.1. Multi-Microgrid System Resilience Enhancement Scheme (Round 1)

In step 1 of this mode, grid-connected microgrids have already performed the local level optimization in the previous interval based on Equations (1)–(13). MG-EMSs have the optimized results for the stored energy in the battery of EVs. EVs parked in the parking lot are asked to take part in the resilience enhancement operation. For those who agree to supply energy, their total stored energy is informed to the CEMS. Equation (19) shows the objective function for the islanded microgrids. The first term of the objective function in Equation (19) shows the DG generation cost and the second term represents the price for buying shortage power from the network. Islanded MG informs its required power along with the price to buy that power to CEMS at each interval during the contingency situation.

$$Min\ C^{DG} \cdot P_t^{DG} + C^{Buy} \cdot P_t^{Short} \quad \forall t \in [t_{cs}, T] \tag{19}$$

Subjected to

$$P_t^{Short} + P_t^{DG} + P_t^{RDG} + P_t^{B-} + \sum_{v=1}^{V} P_{v,t}^{ev-} = P_t^{load} + P_t^{B+} + \sum_{v=1}^{V} P_{v,t}^{ev+} \quad \forall t \in [t_{cs}, T] \tag{20}$$

BESS charging, discharging, and SoC constraints are the same as given in Equations (4)–(7). EVs charging, discharging, and maintenance of SoC are the same as in Equations (8)–(13). Shortage power, the power generated by RDG, power generated from DG, discharging of energy from BESS, and discharged energy from EVs parked at parking lots should be balanced by the electric load, charging of BESS, and charging of parked EV at each interval of time, as represented by (20).

In the second step, the objective of CEMS is to perform global optimization for supplying the energy to the islanded microgrid. After receiving the information from the MG-EMSs in the first step, CEMS performs the optimization. Equation (21) is the objective function, in which the information of the distance ($I_{l \leftarrow k}^{Dis}$) between the microgrids in the network and the amount of energy needed to be supplied ($E_{l \leftarrow k,t}^{Sup}$) by grid-connected microgrids to the islanded microgrid is given. In case, when the islanded microgrids are more than one and available energy is less than the total required energy, energy is proportionally divided among the microgrids.

$$Max \sum_{k=1}^{K} \sum_{\substack{l=1 \\ k \neq l}}^{L} E_{l \leftarrow k,t}^{Sup} \cdot I_{l \leftarrow k}^{Dis} \tag{21}$$

$$\text{where } I_{l \leftarrow k}^{Dis} = 1 - \frac{D_{l \leftarrow k}}{D_{l \leftarrow k}^{max}} \quad \forall I \in [0,1]$$

Subjected to

$$E_{k,t}^{Sup} \leq E_{k,t}^{Avail} \quad \forall k \in K, t \in [t_{cs}, t_{ce}] \tag{22}$$

$$\sum_{k=1}^{K} E_{k,t}^{Sup} \leq E_{l,t}^{Req} \quad \forall k \in K, l \in L, t \in [t_{cs}, t_{ce}] \tag{23}$$

Equation (22) is an energy limit constraint that the grid-connected MGs can supply energy less than or equal to the energy available in EVs. $E_{k,t}^{avail}$ is the total amount of energy stored in EVs in the microgrid that has agreed to supply energy to the islanded microgrid l. Equation (23) shows that the total energy supplied by 'k' microgrids should be less than or equal to the energy requested by l islanded microgrid. The third and last step's objective is to select the minimum and most efficient EVs after getting information from CEMS as shown in Equation (24).

$$Min \sum_{v=1}^{V} Br_{v,t}^{ev} \cdot Eff_{v}^{ev} \tag{24}$$

where $Br_{v,t}^{ev} = [0, 1]$.

Subjected to

$$E_{v,t}^{sup} \leq E_{v,t}^{Std} \quad \forall t \in [t_{cs}, t_{ce}], v \in V \tag{25}$$

$$Br_{v,t}^{ev} = \begin{cases} 1 \ if \ E_{v,t}^{sup} \neq 0 \\ 0 \ else \end{cases} \quad \forall t \in [t_{cs}, t_{ce}], v \in V \tag{26}$$

$$\sum_{EV=1}^{N} E_{v,t}^{sup} = E_{l}^{req} \quad \forall t \in [t_{cs}, t_{ce}], v \in V, l \in L \tag{27}$$

Equation (24) is subjected to the constraints given in Equations (25)–(27). EV can only supply the energy less than or equal to the energy stored in its battery as depicted in Equation (25). Equation (27) is the energy balance equation, EVs will supply energy equal to the energy requested by the islanded MG. EV departure for supplying energy to the islanded MG is subjected to Equation (26), $Br_{v,t}^{ev}$ shows the status of the EV, i.e., 1 for EV going to supply energy and zero otherwise.

3.2.2. Optimization for Grid-Connected Microgrids (Round 2)

After completing the optimization for resilience enhancement operation, grid-connected microgrids can perform the rescheduling at the local level optimization and global level optimization. The decision has been made. in which EVs are going to leave microgrids for resilience enhancement operations. MG-EMSs perform rescheduling for the local level optimization by considering the EVs that are present in the parking lot only. This optimization is performed in the same manner as in the normal mode operation of MG-EMS using Equations (1)–(13), where time $t \in [t_c, T]$. After receiving the information of surplus power and shortage power, CEMS performs global optimization. CEMS performs global optimization for internal and external trading as in normal mode, as shown in Equation (14), subjected to Equations (15)–(18), where time $t \in [t_c, T]$.

The flowchart in Figure 3, summarizes the proposed typical multi-microgrid system's operation step by step for both normal and resilience enhancement modes. The first decision box named *outage* decides the mode of the operation (normal mode or resilience enhancement mode). In normal operation, initially, the optimization is performed by MG-EMS for all microgrids ($N = 3$) at a local level, and then global optimization is performed by the CEMS. On the other hand, in any contingency, MG-EMS performs the optimization for grid-connected and islanded microgrids, and shortage power, surplus power, and required energy by islanded microgrid is informed to CEMS. During this process, the number of grid-connected (n_c) and islanded (n_i) microgrids are updated. After that, CEMS decides which microgrid is going to supply energy to islanded microgrids and update MG-EMS. MG-EMS decides that which EV is going to supply the energy. Finally, rescheduling is performed for the grid-connected microgrids ($N = n_c$) in the case when the outage is still there. When the outage is over, the optimization is performed for all the microgrids ($N = n_c + n_i$) in the network.
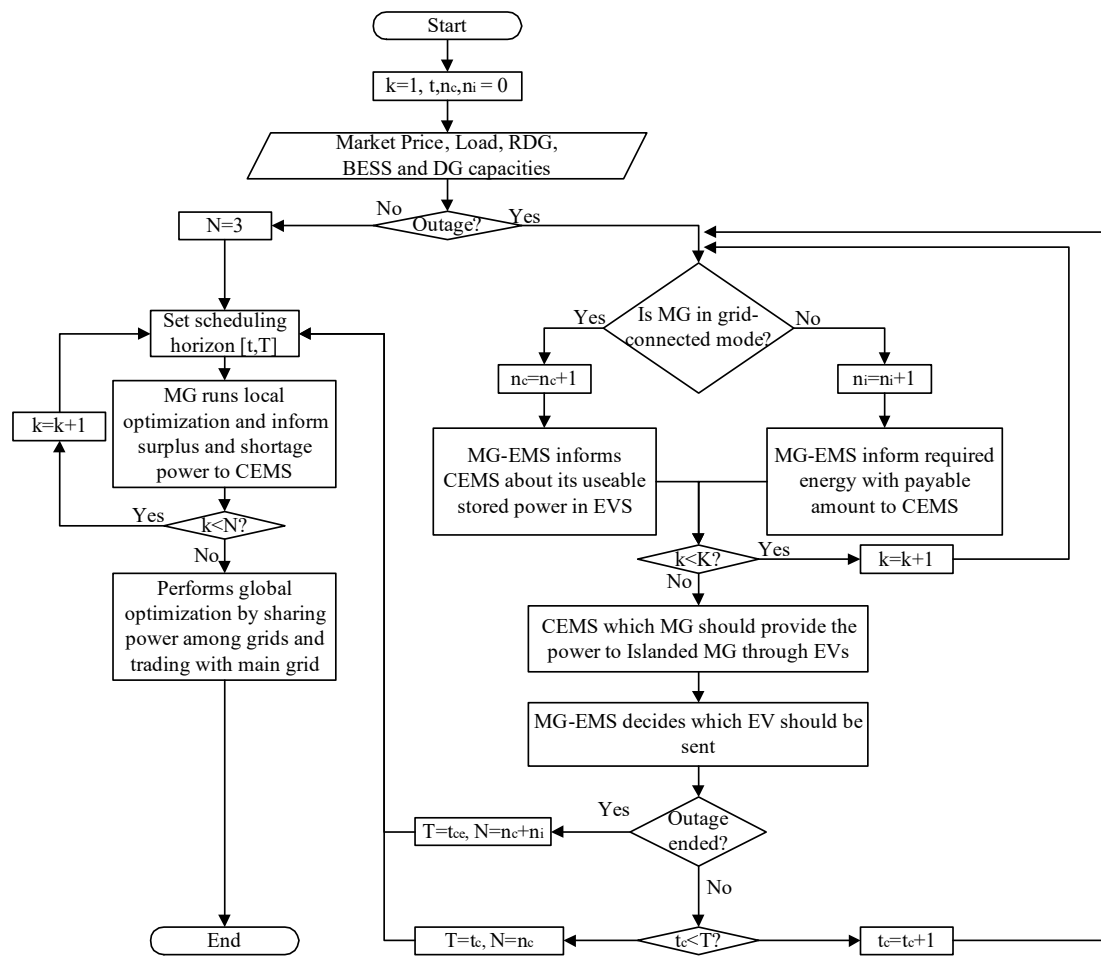
Figure 3. Flowchart for proposed microgrid network operation.

3.2.3. Resilience Index Formulation

In this section, a resilience index has been formulated to evaluate the increase in the resilience of the islanded microgrid with the help of the EVs parked in the parking lot of the microgrids. The resilience of the islanded microgrid is computed by using the survived load without EVs and survival load with EVs of the islanded microgrid as depicted by Equation (28). Survival load without EVs is the energy supplied to survive load with local resources available in the islanded microgrid, while survival load with EVs is the total load survived with EVs and local resources.

$$I^{Res} = \left(1 - \frac{L_{Sur}^{wo\_EVs}}{L_{Sur}^{w\_EVs}} \right) \times 100 \tag{28}$$

4. Numerical Simulation

A multi-microgrid system, as shown in Figure 1, is operated over a 48-h scheduling horizon with a time interval of 1 h (*t*). The proposed multi-microgrid network can operate in both normal and resilience enhancement modes. The system initially operates in the normal mode while in the case of any contingency, it can switch to the resilience enhancement mode. For normal mode, MG-EMSs and CEMS optimization results for 48 h intervals have been simulated and studied, and to analyze the performance of the resilience enhancement mode, three different cases have been simulated under different conditions. Simulations for the study have been conducted in Microsoft Visual Studio by using CPLEX 12.7.1 [27].

4.1. Input Parameters

In this study, we have considered three microgrids in the multi-microgrid system. MG1, MG2, and MG3 are residential, commercial, and industrial MGs, respectively. Three different MGs are selected to make sure that EVs are available throughout the day in the parking lot for resilience purposes. In the case when EVs are not available in the parking lot or non agree to supply energy, the energy stored in the battery energy storage system and local generation resources are used to supply energy to the system. The distance between MG1-MG2, MG2-MG3, and MG1-MG3 is 8 km, 5 km, and 10 km, respectively. Load profiles of MGs are taken from [28–30] and are scaled, as given in Figure 4. The time-of-use (TOU) market price signals are used as in [31] and are shown in Figure 5. Charging and discharging efficiencies and capacity of BESS for each MG are given in Table 1. Table 2 shows the parameters for distributed generators inside the microgrids. Table 3 shows the capacities and efficiencies (energy consumption per km). EV ID in Table 3 is the ID allocated to each EV to identify them e.g., the Mini Cooper has an ID 3 in MG1 while ID 1 in MG2. Arrival and departure time details are given in Table 4. EV charging and discharging efficiencies are chosen between a range of 94% to 96% and targeted SoC (SoC^{ev}_{v,t^d}) is set to maximum SoC of EV. The initial SoC of EVs is randomly chosen between a range of 25% to 40% of battery capacity. The data for EVs capacities and efficiencies are taken from [32,33], respectively. RDGs output power in MGs is taken from [34] and is scaled, shown in Figure 6.
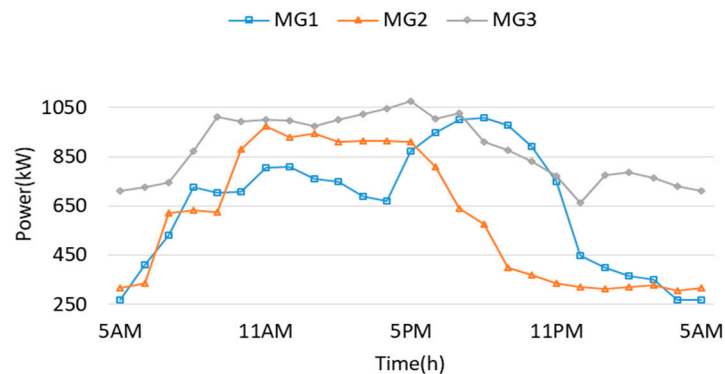

Figure 4. Load profile of the microgrids.

Figure 5. Time-of-use (TOU) market price signals.

Table 1. Battery energy storage system (BESS) input parameters.

Parameters	Capacity (kWh)	Charging Efficiency (%)	Discharging Efficiency (%)	Initial SOC (%)
MG1-BESS	200	95	95	50
MG2-BESS	100	95	95	50
MG3-BESS	150	95	95	50

Table 2. Input parameters for distributed generation.

Parameters	Capacity (kW)	Cost (KRW/kWh)
MG1-DG	700	75
MG2- DG	600	102
MG3- DG	550	110

Table 3. EVs BESS capacities and availability in microgrids (MGs).

EV	Capacity (kW)	Efficiency (W/km)	EV ID		
			MG1	MG2	MG2
Hyundai IONIQ Electric	38.3	153	1	9,14	-
Tesla Model 3 Std. Range Plus	47.5	153	2	10,15	-
Mini Cooper SE	28.9	256	3	1	-
BMW i3 120 Ah	37.9	161	4.11	2	4
Kia e-Soul 39 kWh	39.2	170	5.12	3	5
Nissan Leaf e+	56	172	6.13	4	6
Lexus UX 300e	52	193	7.14	-	7
Ford Mustang Mach-E GT	88	215	8.15	12	8
Audi e-Tron 50 Quattro	64.7	231	9	13	9
Jaguar I-Pace EV400	84.7	232	10	7	10
Porsche Taycan Turbo	83.7	209	-	8	3
Audi Q4 e-Tron*	77	193	-	11	1
BMW iX3	74	206	-	-	2
Honda e Advance	28.5	168	-	5	-
Volkswagen e-Golf	38	168	-	6	-

Table 4. Electric vehicles (EVs) arrival and departure timings.

| EV ID	MG1		MG2		MG3	
	Departure Time	Arrival Time	Arrival Time	Departure Time	Arrival Time	Departure Time
1	8 AM	6 PM	7 AM	4 PM	10 AM	6 PM
2	10 AM	8 PM	8 AM	4 PM	9 AM	8 PM
3	9 AM	9 PM	9 AM	4 PM	8 AM	8 PM
4	8 AM	7 PM	8 AM	5 PM	8 AM	4 PM
5	6 AM	9 PM	9 AM	5 PM	8 AM	4 PM
6	8 AM	5 PM	11 AM	9 PM	9 AM	4 PM
7	8 AM	7 PM	9 AM	6 PM	8 AM	5 PM
8	9 AM	4 PM	10 AM	8 PM	9 AM	5 PM
9	12 PM	7 PM	9 AM	6 PM	11 AM	9 PM
10	9 AM	8 PM	10 AM	6 PM	9 AM	6 PM
11	10 AM	6 PM	7 AM	7 PM	-	-
12	8 AM	8 PM	8 AM	7 PM	-	-
13	12 PM	7 PM	7 AM	7 PM	-	-
14	7 AM	6 PM	9 AM	8 PM	-	-
15	9 AM	8 PM	11 AM	8 PM	-	-
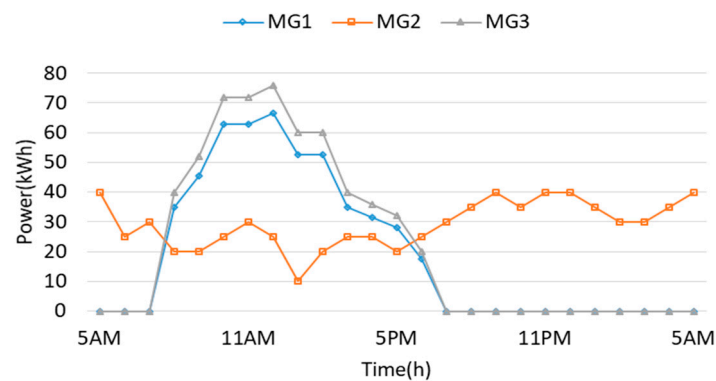
Figure 6. Renewable distributed generations (RDGs) output power profile.

4.2. Normal Mode

In this section, optimized results for both MG-EMS and CEMS are analyzed. During this mode, the multi-microgrid network is working normally and the microgrids can trade power with the utility grid.
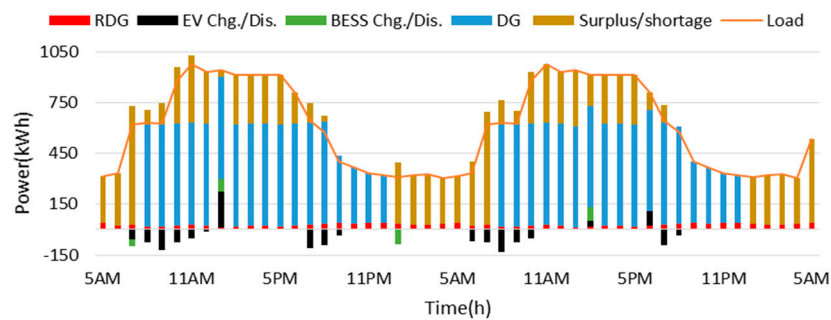
4.2.1. Microgrid Energy Management System

Figure 7a shows the results for the power balance in MG1 at each interval *t*. It can be observed that DG being the cheaper source, generates power throughout the day. BESS is charged from the DG at off-peak intervals and discharged at the peak intervals. EVs are mainly charged from the DG at off-peak intervals, except during 6 PM of day 1 and 5,6,7 PM of day 2, where few EVs are charged at peak intervals to store the targeted SoC in batteries of EVs for resilience purposes because on the arrival time, EVs batteries have less energy than the energy required for resilience purposes. When the selling price is higher than the generation price of DG, DG generates surplus power. When the load is greater than the maximum generation capacity of DG, shortage power is either bought from the utility grid or received from neighboring microgrids and this decision is made by CEMS. Moreover, RDG is providing power only during day time.

Figure 7b shows the results for the local level optimization of MG2. RDGs constitute wind turbines, providing free energy throughout the day. DG operates between 8 AM to 12 AM, while BESS is charged in intervals when the market price is low and discharged when the market price is high. On the arrival of EVs to the parking lot, EVs are charged to their targeted SoC because of the increasing behavior of the market price. EVs arriving in the off-peak interval (in the morning) in the parking lot and departing in the off-peak interval (in the late evening) are discharging energy during peak intervals on the day (1 PM of day 1 and 2 PM and 6 PM of day 2).

Figure 7c shows the local level optimization results of MG3 where RDG are photovoltaic cells, therefore they generate power only during the day time. MG3 DG is the most expensive of all, that's why it is generating power only during peak price intervals. BESS is charged during off-peak intervals and discharged during peak intervals. EVs that arrived before midday are charged as soon as they in the parking lot while remaining are charged when the market price is decreased again before EVs departure. During off-peak intervals and higher load intervals, power is bought from the utility grid and/or received from other microgrids in the multi-microgrid system.
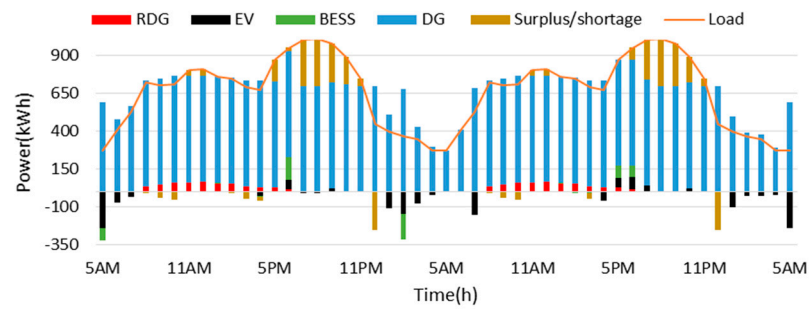
(**a**)

(**b**)
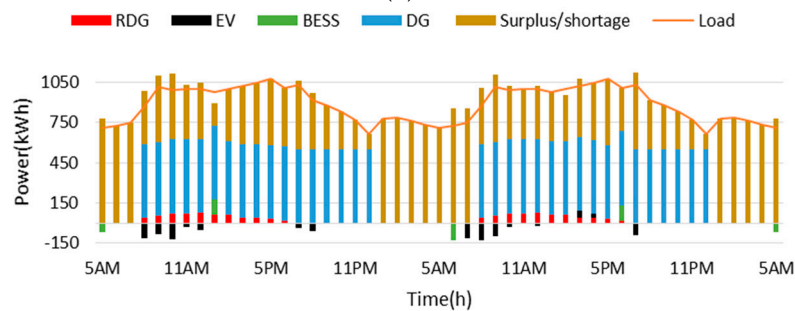
(**c**)

Figure 7. Microgrid power balance of: (**a**) MG1; (**b**) MG2; (**c**) MG3.

4.2.2. Central Energy Management System

CEMS receives the information of surplus power and shortage power from each microgrid as shown in Figure 7. CEMS decides either to share the power among microgrids or to trade with the utility grid. In this case study, only MG1 has Surplus power which is shared proportionally among other microgrids as shown in Figure 8a. The remaining surplus or shortage power after internal trading is traded with the utility grid as shown in Figure 8b. After this step, the multi-microgrid system is now globally optimal.
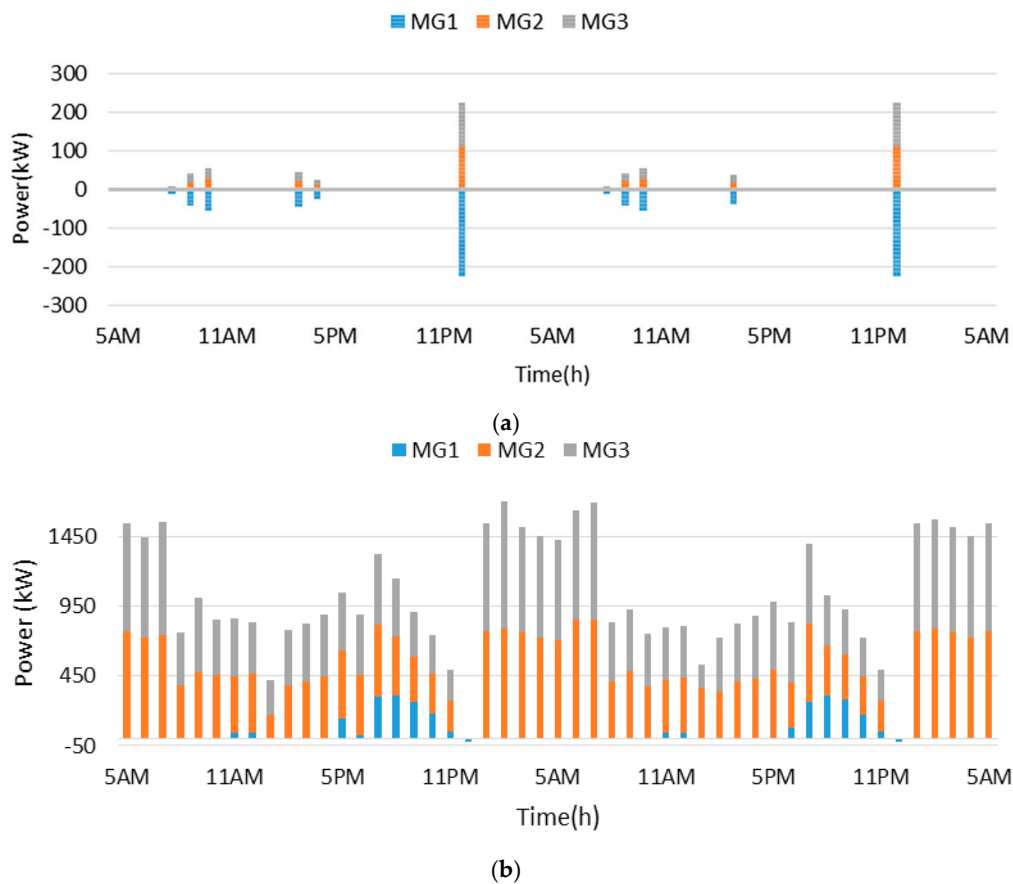
Figure 8. Central energy management system (CEMS) results: (**a**) Internal trading among microgrids; (**b**) External trading of networked microgrids with the utility grid.

4.3. Resilience Enhancement Mode

4.3.1. Local Level Optimization (Round 1: Step 1)

During this step, it has been assumed that the MG3 has lost its power connection with other microgrids, based on the available number of EVs (parked in the parking lot of that microgrid at that time). To analyze the effectiveness of the proposed method, three different cases have been studied. Table 5 shows the input data received by CEMS after step 1 from the grid-connected microgrids (MG1 and MG2) and the islanded microgrid (MG3) for these cases. Figure 9 shows the total energy stored in the EVs parked in the parking lot of grid-connected microgrids. These results are formulated after the optimization performed in the last hour.

Table 5. Input data for cases.

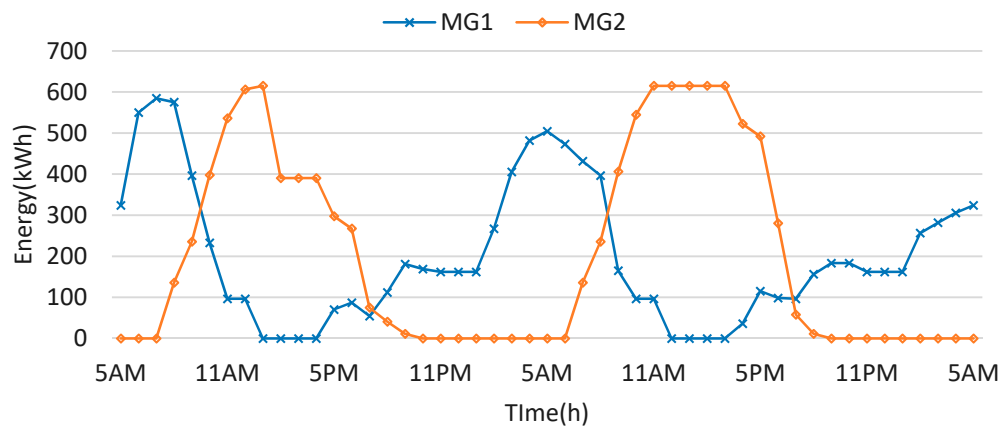| Cases	Time/Day	MG3 Required (kWh)	Available Energy	
			MG1 (kWh)	MG2 (kWh)
1	6 AM/1	61	262.56	0
2	8 AM/1	168	206	67.2
3	2 AM/1	212	306	0

Figure 9. Maximum available energy stored in EVs parked in the microgrids.

4.3.2. Central Level Optimization (Round 1: Step 2)

After the completion of step 1, CEMS decides to supply the energy to the islanded microgrid (MG3). Figure 10 shows the results for all three cases at the CEMS level after step 1. It can be observed in case 1 that MG1 (grid-connected) supplies energy to the islanded microgrid (MG3). At that time, only MG1 has energy availability because of the parked EVs in the parking lot as illustrated in Figure 9 (at 6 AM, day 1). In case 2, MG1 and MG2 have energy availability as shown in Figure 9 (at 8 AM, day 1), therefore, MG2 being closer to MG3 (5 km away) supplies all of its available energy through EVs (67.2 kWh), and the remaining energy (100.8 kWh) is supplied by EVs parked in the parking lot of MG1 (8 km away). In case 3, MG3 can only generate power through DG, therefore the remaining power is supplied by EVs of MG1 at (at 2 AM, day 1) because there is no power from RDGs (RDGs are photovoltaic cells) and BESS is also empty.
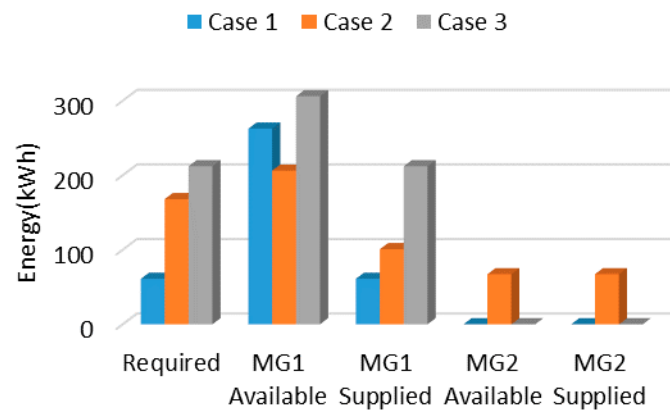

Figure 10. CEMS decision after round 1: step 2.

4.3.3. Local Level Optimization (Round 1: Step 3)

After the completion of optimization at the CEMS level in step 2, MG-EMS for each microgrid has to decide which EV should be sent. In Figures 11–13, EVs parked in the parking lot are shown, e.g., in Figure 12b, EVs with ID 10,14,15 are parked in the parking lot. In case 1, MG-EMS has all EVs parked in its parking lot, and it has been assumed that among them only 5 have agreed to supply energy as shown in Figure 11. Therefore, EV 8 is selected by MG-EMS because it is the most efficient EV among the agreed ones. Even though EV 10 can also supply the energy, EV 8 is more efficient in consuming energy while traveling as given in Table 4. Figure 12a, b shows the optimized results for case 2, MG2 being closer to MG3, supplies the energy through EV 10 as shown in Figure 12b,

while remaining energy is supplied by MG1 to MG3 through EV 2 and 8, among the agreed ones as shown in Figure 12a. In case 3, MG1 supplies energy to MG3 to fulfill its load demands as shown in Figure 13. Four out of 7 agreed EVs (EV ID 2,10,13,15) are going to supply energy to the islanded microgrid. With the proposed strategy, there is a considerable increase in the resilience of the islanded microgrid varying from 8.41% in case 1 to 27.8% in case 3, as shown in Table 6.
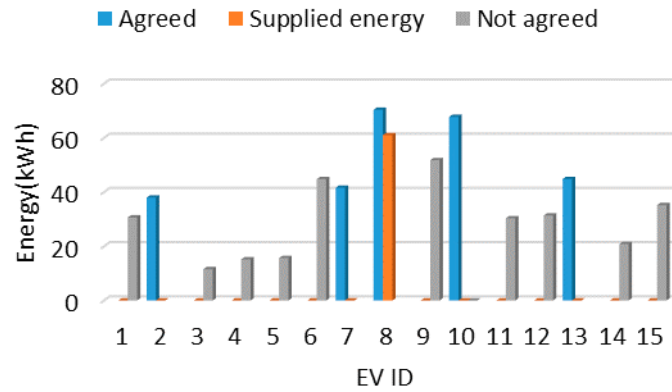

Figure 11. Microgrid energy management systems (MG-EMSs) decision of EVs for case 1.
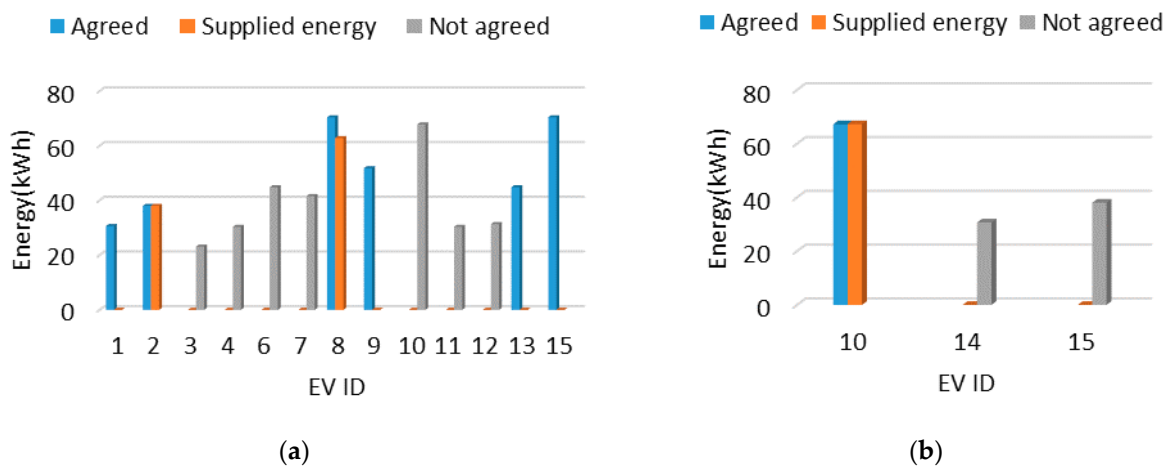

(**a**)   (**b**)

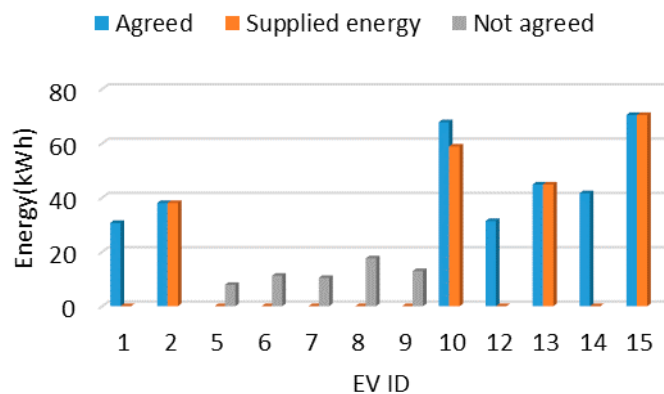**Figure 12.** MG-EMS decision of EVs for case 2: (**a**) MG1; (**b**) MG2.

Figure 13. MG-EMS decision for EVs case 3.

Table 6. Increase in the resilience of islanded microgrids with the proposed strategy.

Cases	Load Survived without EVs (kWh)	Load Survived with EVs (kWh)	Resilience Increase (%)
1	664	725	8.41
2	704.5	872.5	9.25
3	550.5	762.5	27.8

4.3.4. Local Level Optimization (Round 2: Step 1)

In step 1, grid-connected microgrids (MG1 and MG2) decide to reschedule the components from time interval t_c to time T. Rescheduling in step 1 of round 2 is the same as the MG-EMS optimization at the local level in normal mode. The rescheduling results of only case 3 are shown due to space limitations. Figure 14a shows the MG-EMS optimization for MG1 at the local level. As in the normal mode, all the components of the microgrids are working in the same way. EVs leaving the microgrid parking lot for supplying energy to islanded microgrid (MG3) arrive back and are charged at 4 AM. MG2 results are the same as in the normal mode, shown in Figure 14b.
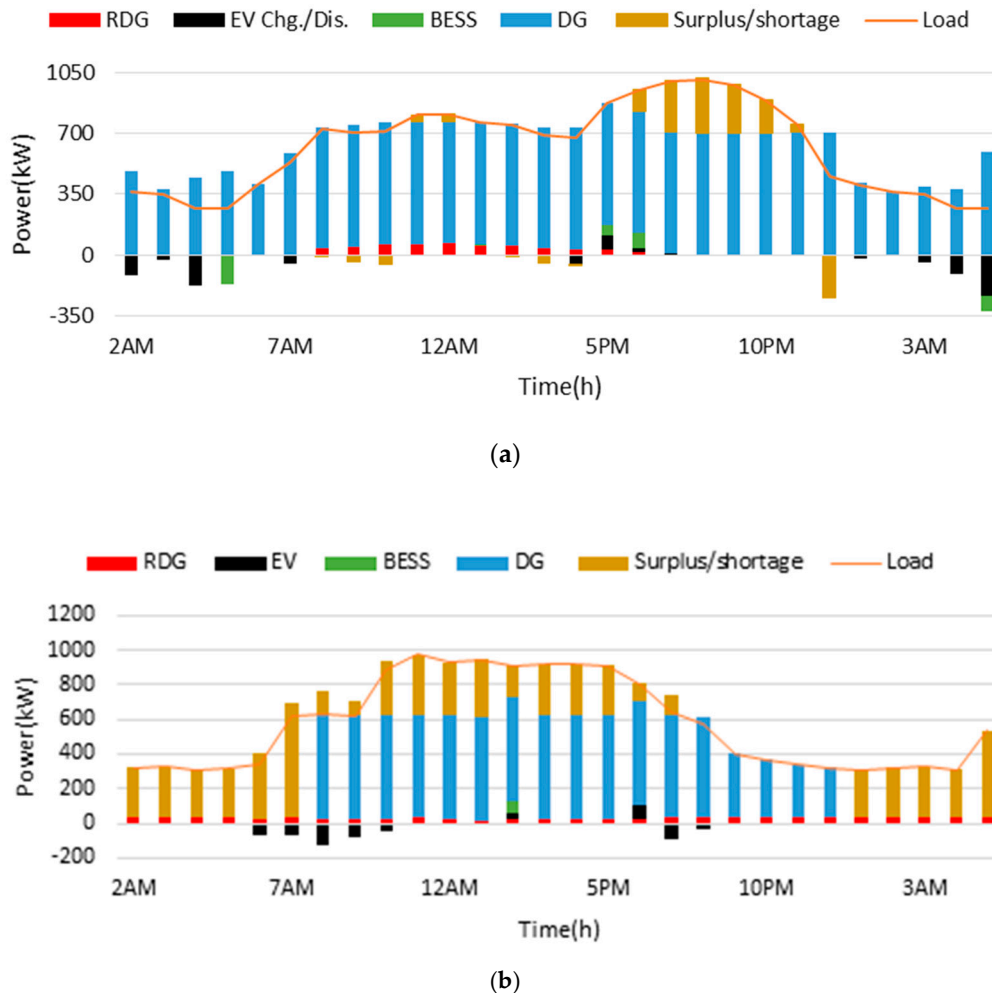

(**a**)

(**b**)

Figure 14. Microgrid rescheduling results: (**a**) MG1; (**b**) MG2.

4.3.5. Central Level Optimization (Round 2: Step 2)

After completion of rescheduling of MG-EMS in step 1, CEMS receives the information for the global optimization of the multi-microgrid system. Figure 15a shows the results

for the internal trading among microgrids after step 2. Surplus power of MG1 at the intervals 8–10 AM and 2–4 PM is supplied to MG2. The remaining surplus power/shortage power after internal trading is sold/bought to/from the utility grid as shown in Figure 15b. After the rescheduling in step 2, the multi-microgrid system is now globally optimal.
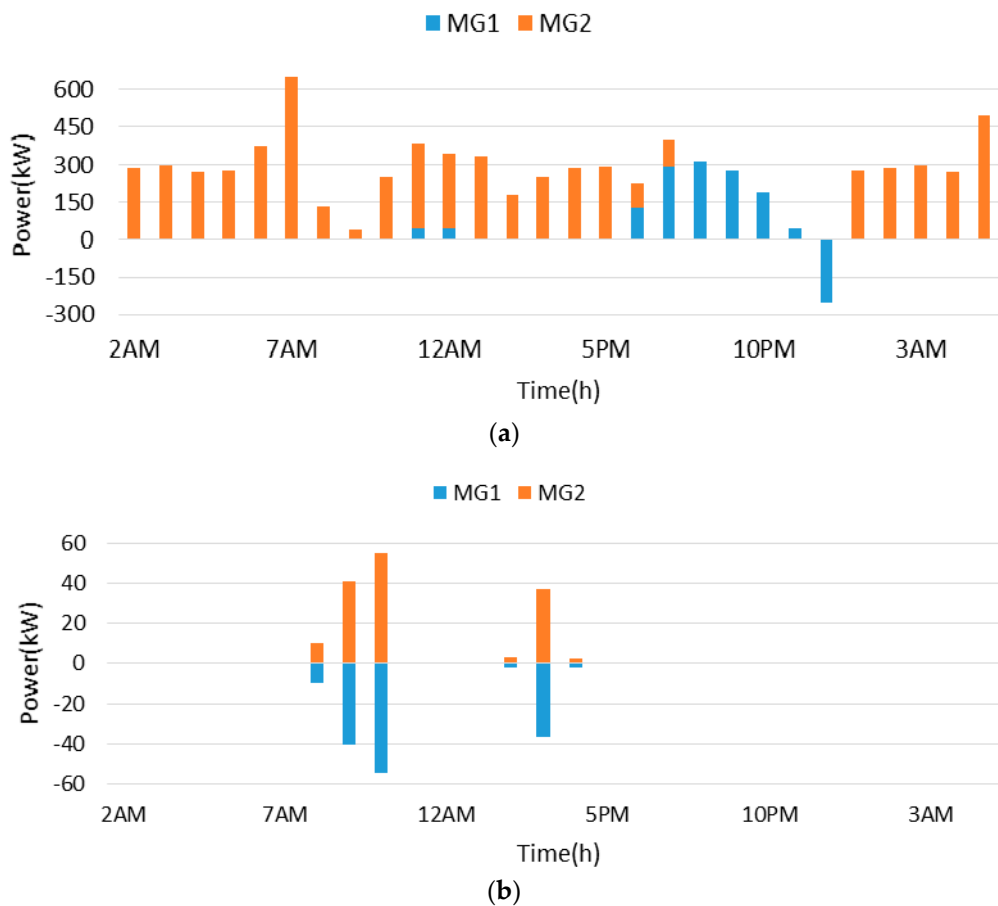

(a)

(b)

Figure 15. Rescheduled results of CEMS: (**a**) Internal trading among grid-connected microgrids; (**b**) External trading of networked microgrids with the utility grid.

5. Conclusions

In this study, an algorithm for the resilience enhancement of the multi-microgrid system along with the normal operation of the microgrid has been proposed. Initially, normal mode results have been simulated to show the optimized operation of networked microgrids without any contingency. During the resilience enhancement mode, in the case of any contingency, electric vehicles parked in the parking lot of grid-connected microgrids are sent to the islanded microgrid to fulfill the needs of electric loads. The existing electric vehicles in the microgrids can be utilized to enhance the resilience of microgrids which will increase the profit for electric vehicle owners without the requirement of additional investment cost for the microgrid operators. Simulation results have shown that the proposed algorithm is capable of providing power to islanded microgrids for surviving critical loads without any direct power connection between the microgrids.

Author Contributions: A.Y.A.; conceived and designed the experiments, A.Y.A. and A.H.; performed the experiments and analyzed the data, H.-M.K.; revised and analyzed the results, J.-W.B.; project administration and resources, A.Y.A.; wrote the paper. All authors have read and agreed to the published version of the manuscript.

Conflicts of Interest: The authors declare no conflict of interest.

Nomenclature

Identifiers and Binary Variables

t	Index of time, running from 1 to T
t_c	Time at which contingency/outage occurred
k, l	Index of microgrids, running from 1 to M and 1 to N, respectively
$I^{Dis}_{l \leftarrow k}$	Index of distance from microgrid k to l
$Br^{ev}_{v,t}$	Status indicator of vehicle v for supplying energy
I^{Res}	Index of resilience

Variables and Constants

C^{DG}	Production cost of dispatchable generator.
C^{GB}_t, C^{GS}_t	The price for buying and selling power to/from the utility grid at time t.
$P^{DG}_{min}, P^{DG}_{max}$	Minimum and maximum generation capacity of the dispatchable generator.
P^{Short}_t, P^{Sur}_t	Shortage and surplus power in a microgrid at time t.
P^{RDG}_t	The forecasted output power of renewable distributed generation of at time t.
P^{Load}_t	Forecasted load of a microgrid at time t.
P^{B-}_t, P^{B+}_t	Charging and discharging of BESS at time t.
$P^{ev-}_{v,t}, P^{ev+}_{v,t}$	Charging and discharging of vehicle v at time t.
$SoC^B_t, SoC^{ev}_{v,t}$	SoC of BESS and vehicle v at time t, respectively.
P^{cap}_B, P^{cap}_v	Capacity of BESS and vehicle v, respectively.
η^c, η^d	Charging and discharging efficiency of BESS, respectively.
η^{ev+}, η^{ev-}	Charging and discharging efficiency of vehicle v, respectively.
SoC^{exit}_{v,t^d}	Targeted SoC of vehicle v at departure time.
E^{res}	Energy stored for resilience in the battery of vehicle while parked at parking lot.
$P^{Send}_{k \rightarrow l,t}$	Energy sent from microgrid k to l at time t.
$P^{Rec}_{l \leftarrow k,t}$	Energy received by microgrid l form k at time t.
$P^{T\_Sur}_t, P^{T\_Short}_t$	Total surplus and shortage power in the system at time t, respectively.
$E^{Sup}_{l \leftarrow k,t}$	Energy supplied by microgrid k to l at time t.
$E^{Avail}_{k,t}$	Energy available in microgrid k at time t.
$E^{Req}_{l,t}$	Energy requested by microgrid l at time t.
Eff^{ev}_v	Per km energy consumption efficiency of vehicle v.
$E^{sup}_{v,t}, E^{std}_{v,t}$	Energy supplied and energy stored in vehicle v at time t, respectively.
$L^{w\_EVs}_{Sur}, L^{wo\_EVs}_{Sur}$	Islanded microgrid survived load with and without EVs in the case of contingency, respectively.

References

1. Saman, N.; Kamran, J.; Ehsan, K.; Gevork, B.G. Optimal wind turbine allocation and network reconfiguration for enhancing resiliency of system after major faults caused by natural disaster considering uncertainty. *IET Renew. Power Gen.* **2018**, *12*, 1413–1423.
2. Mathaios, P.; Pierluigi, M. Influence of extreme weather and climate change on the resilience of power systems: Impacts and possible mitigation strategies. *Electr. Power Syst. Res.* **2015**, *127*, 259–270.
3. Motyka, M.; Slaugthter, A.; Berg, J. Reinventing Resilience: Defining the Model for Utility-Led Renewable Microgrids. 2016. Available online: https://www2.deloitte.com/content/dam/Deloitte/us/Documents/energy-resources/us-er-reinventing-resilience-microgrid.pdf (accessed on 23 November 2020).
4. Panteli, M.; Mancarella, P. The grid: Stronger, bigger, smarter? Presenting a conceptual framework of power system resilience. *IEEE Power Energy Mag.* **2015**, *13*, 58–66. [CrossRef]
5. Huang, G.; Wang, J.; Chen, C.; Qi, J.; Guo, C. Integration of preventive and emergency responses for power grid resilience enhancement. *IEEE Trans. Power Syst.* **2017**, *32*, 4451–4463. [CrossRef]

6. Hussain, A.; Aslam, M.; Syed, M.A. A standards-based approach for auto-drawing single line diagram of multivendor smart distribution systems. *Int. J. Electr. Power Energy Syst.* **2018**, *96*, 357–367. [CrossRef]
7. Panteli, M.; Trakas, D.N.; Mancarella, P.; Hatziargyriou, N.D. Boosting the power grid resilience to extreme weather events using defensive islanding. *IEEE Trans. Smart Grid* **2016**, *7*, 2913–2922. [CrossRef]
8. Wang, X.; Li, Z.; Shahidehpour, M.; Jiang, C. Robust line hardening strategies for improving the resilience of distribution systems with variable renewable resources. *IEEE Trans. Sustain. Energy* **2019**, *10*, 386–395. [CrossRef]
9. Ali, H.; Hussain, A.; Bui, V.-H.; Jeon, J.; Kim, H.-M. Welfare maximization-based distributed demand response for islanded multi-microgrid networks using diffusion strategy. *Energies* **2019**, *12*, 3701. [CrossRef]
10. Ali, H.; Hussain, A.; Bui, V.-H.; Kim, H.-M. Consensus algorithm-based distributed operation of microgrids during grid-connected and islanded modes. *IEEE Access* **2020**, *8*, 78151–78165. [CrossRef]
11. Bahramirad, S.; Khodaei, A.; Svachula, J.; Aguero, J.R. Building resilient integrated grids: One neighborhood at a time. *IEEE Electrif. Mag.* **2015**, *3*, 48–55. [CrossRef]
12. Qi, H.; Wang, X.; Tolbert, L.M.; Li, F.; Peng, F.Z.; Ning, P.; Amin, M. A resilient real-time system design for a secure and reconfigurable power grid. *IEEE Trans. Smart Grid* **2011**, *2*, 770–781. [CrossRef]
13. Pashajavid, E.; Shahnia, F.; Ghosh, A. Resilient Distribution Systems with Community Microgrids. Ph.D. Thesis, Ohio State University, Columbus, OH, USA, 2016. Available online: https://www.researchgate.net/publication/317969135_Resilient_Distribution_Systems_With_Community_Microgrids (accessed on 23 November 2020).
14. Li, Z.; Shahidehpour, M.; Aminifar, F.; Alabdulwahab, A.; Al-Turki, Y. Networked microgrids for enhancing the power system resilience. *Proc. IEEE* **2017**, *105*, 1289–1310. [CrossRef]
15. Rosales, E.; Simón-Martín, M.; Borge-Diez, D.; Blanes, J.; Colmenar-Santos, A. Microgrids with energy storage systems as a means to increase power resilience: An application to office buildings. *Energy* **2019**, *172*, 1005–1015. [CrossRef]
16. Mayank, P.; Sayonsom, C.; Manish, M.; Yusheng, L.; Fernando, D.; Rob, H.; Anurag, K.S. Integration of flow battery for resilience enhancement of advanced distribution grids. *Int. J. Electr. Power Energy Syst.* **2019**, *109*, 314–324.
17. Tian, M.W.; Pouyan, T. Energy cost and efficiency analysis of building resilience against power outage by shared parking station for electric vehicles and demand response program. *Energy* **2021**, *215*, 119058. [CrossRef]
18. Kim, J.; Dvorkin, Y. Enhancing distribution system resilience with mobile energy storage and microgrids. *IEEE Trans. Smart Grid* **2019**, *10*, 4996–5006. [CrossRef]
19. Kim, J.; Dvorkin, Y. Enhancing distribution resilience with mobile energy storage: A progressive hedging approach. In Proceedings of the IEEE Power & Energy Society General Meeting (PESGM), Portland, Oregon, 5–10 August 2018; pp. 1–5.
20. Gouveia, C.; Moreira, J.; Moreira, C.L.; Peças Lopes, J.A. Coordinating storage and demand response for microgrid emergency operation. *IEEE Trans. Smart Grid* **2013**, *4*, 1898–1908. [CrossRef]
21. Global EV Outlook 2019. Available online: https://www.iea.org/reports/global-ev-outlook-2019:2020 (accessed on 23 November 2020).
22. Hossein, A.; Peyman, B. A contingency based energy management strategy for multi-microgrids considering battery energy storage systems and electric vehicles. *J. Energy Storage* **2020**, *27*, 101087.
23. Peças Lopes, J.A.; Silvan, A.; Polenz, C.L.; Moreira, R.C. Identification of control and management strategies for LV unbalanced microgrids with plugged-in electric vehicles. *Electr. Power Syst. Res.* **2010**, *80*, 898–906. [CrossRef]
24. Bui, V.H.; Hussain, A.; Kim, H.M. A multiagent-based hierarchical energy management strategy for multi-microgrids considering adjustable power and demand response. *IEEE Trans. Smart Grid* **2018**, *9*, 1323–1333. [CrossRef]
25. Li, K.; Tseng, K.J. Energy Efficiency of Lithium-Ion Battery Used as Energy Storage Devices in Micro-Grid. In Proceedings of the IECON 2015-41st Annual Conference of the IEEE Industrial Electronics Society, Yokohama, Japan, 9–12 November 2015; pp. 5235–5240.
26. Hussain, A.; Bui, V.H.; Kim, H.M. A proactive and survivability-constrained operation strategy for enhancing resilience of microgrids using energy storage system. *IEEE Access* **2018**, *6*, 75495–75507. [CrossRef]
27. *ILOG CPLEX 12.7.0 Users Manual*; ILOG SA: Gentilly, France, 2016.
28. Ferruzzi, G.; Graditi, G.; Rossi, F.; Russo, A. Optimal operation of a residential microgrid: The role of demand side management. *Intell Ind. Syst.* **2015**, *1*, 61–82. [CrossRef]
29. He, L.; Liu, N. Load Profile Analysis for Commercial Buildings Microgrids under Demand Response. In Proceedings of the IEEE Conference on Industrial Electronics and Applications (ICIEA), Siem Reap, Cambodia, 18–20 June 2017; pp. 461–465.
30. Mirzaei, M.; Vahidi, B. Feasibility analysis and optimal planning of renewable energy systems for industrial loads of a dairy factory. *J. Renew. Sustain. Energy* **2015**, *7*, 063114. [CrossRef]
31. Hussain, A.; Bui, V.H.; Kim, H.M. Optimalsizing of battery energy storage system in a fast EV charging station considering power outages. *IEEE Trans. Transp. Electrif.* **2020**, *6*, 453–463. [CrossRef]
32. Energy Consumption of Full Electric Vehicles. Available online: https://ev-database.org/cheatsheet/energy--consumption-electric-car:2020 (accessed on 23 November 2020).
33. Useable Battery Capacity of Electric Vehicles. Available online: https://ev-database.org/cheatsheet/useable-battery-capacity-electric-car:2020 (accessed on 23 November 2020).
34. Bui, V.H.; Hussain, A.; Kim, H.M. Double deep Q -learning-based distributed operation of battery energy storage system considering uncertainties. *IEEE Trans. Smart Grid* **2020**, *11*, 457–469. [CrossRef]